Teknomekanik, Vol. 8, No. 2, pp. 136-163, December 2025
e-ISSN: 2621-8720 p-ISSN: 2621-9980

Performance analysis of soybean oil with CuO/Graphene hybrid additive nanoparticles as cutting fluid on CNC machining processes

Agus Setiawan[1*], Poppy Puspitasari[2], Mohammad Tauviqirrahman[3], Diki Dwi Pramono[4] and Haipan Salam[5]

[1] Mechanical Engineering Education Study Program, Universitas Pendidikan Indonesia, **Indonesia**
[2] Department of Mechanical and Industrial Engineering, Universitas Negeri Malang, **Indonesia**
[3] Department of Mechanical Engineering, Faculty of Engineering, Universitas Diponegoro, **Indonesia**
[4] Centre of Advanced Material and Renewable Energy, Universitas Negeri Malang, **Indonesia**
[5] Chemical Engineering Study Program, Universitas Pendidikan Indonesia, **Indonesia**

* Corresponding Author: agus_setiawan@upi.edu
Received: 25 June 2025; *Revised:* 20 August 2025; *Accepted:* 05 October 2025

Cite this https://doi.org/10.24036/teknomekanik.v8i2.42472

Abstract: This study investigates the performance of soybean oil-based nano-lubricants with CuO, graphene, and CuO/graphene hybrids under MQL-assisted CNC milling of AISI 1045 steel. The research aims to evaluate the thermophysical, rheological, and tribological properties of various lubricant formulations, including pure soybean oil and soybean oil with individual or hybrid nanoparticle additives. Nanoparticles were characterized by SEM, XRD, and FTIR, and fluid samples were evaluated for density, viscosity, thermal conductivity, sedimentation stability, and rheological behavior. Machining performance was assessed through tool wear, surface roughness, cutting temperature, wear debris morphology, and chip color analysis. Results showed that adding graphene nanoparticles significantly improved machining performance, achieving a surface roughness of 1.033 µm, tool wear of 0.0493 mm, and a cutting temperature of 46.1 °C, outperforming both conventional and alternative nanofluid formulations. Among all formulations, the graphene-based nanofluid delivered the lowest cutting temperature, surface roughness, and flank wear under MQL. The CuO/graphene hybrid improved performance relative to the base fluids but did not surpass the graphene formulation, indicating limited synergistic benefits under the present soybean oil-based-MQL conditions.

Keywords: biolubricant; nanolubricant; minimum quantity lubrication; CNC milling; eco-friendly cutting fluid

1. Introduction

Computer numerical control (CNC) machines are widely applied across manufacturing sectors owing to their technological sophistication. Milling machines, in particular, are common in mold making, automotive, and aerospace industries because of their high efficiency and superior surface quality [1], [2]. AISI 1045 steel is a mediums-carbon steel widely used due to its machinability, strength, toughness, ductility, and material availability [3]. During milling of AISI 1045 steel, high temperature and pressure in the cutting zone cause friction-induced tool wear, thermal fatigue, and reduced tool life, leading to substantial production losses [4]. These problems must be reduced because friction and surface wear will have a significant impact on components, with approximately 80% leading to workpiece failure and production process issues [5]. Therefore, lubrication and cooling are needed to reduce friction in the cutting area [4]. The function of lubricants and coolants is to reduce friction, pressure, and heat on the surface of the tool and workpiece, remove chip impurities, improve performance effectiveness, and prevent workpiece corrosion. Lubricants are usually made from mineral oil-based cutting fluids and flooding methods.

Flooded mineral-oil-based cutting fluids are commonly employed to reduce high cutting temperatures during machining. However, only a small portion reaches the cutting zone, limiting its cooling and lubricating effectiveness [6], [7]. Additionally, extensive and significant use of the flooding method will increase production costs [8], [9], [10], [11]. In addition, conventional mineral-oil-based cutting fluids cause environmental pollution and pose risks to human health [12], [13]; while mineral-oil resources are steadily depleting [14]. Therefore, milling processes must align with green-machining principles to achieve sustainable advancement and address these challenges. Recent studies also note that replacing mineral oil with alternatives is not sufficient; the fluids must also sustain thermal stability and machining efficiency under severe cutting conditions, which remains a challenge [15].

Vegetable-oil-based cutting fluids are increasingly popular owing to their non-toxicity [16], high biodegradability, renewability, cost-effectiveness [17], and abundant natural availability [18]. Araújo et al. [19] evaluated and compared edible vegetable oils (corn, cottonseed, babassu bean, canola, sunflower, and soybean oils) with non-edible vegetable oil LB2000 in milling machining of AISI 1045 steel. The results demonstrated excellent lubricating performance across all tested vegetable oils. Soybean oil has better lubricating properties and biodegradability than mineral oil for machining applications [20]. The disadvantages of using soybean oil as a lubricant include its high oxidative instability, low viscosity at high temperatures, and a limited temperature range during application [21]. To address these issues, a mixture of soybean oil and nanomaterials is used to enhance its performance.

Minimum Quantity Lubrication (MQL), also known as near-dry machining, microlubrication, or mist cooling, is an environmentally friendly and efficient machining technique increasingly adopted to enhance performance [22]. The principle of MQL involves only a small amount of cutting fluid (6-100 ml/h), which is sprayed in combination with compressed gas at 4-6 bar in the machining area [23]. The high-pressure gas assists in cooling and chip removal while ensuring that the sprayed fluid forms a thin lubricating film on the cutting surface for optimal performance [24], [25]. Moreover, MQL is far more fluid-efficient than the conventional flooding method (1200 L/h), resulting in a cleaner cutting zone and greater machining efficiency [26], so that by using this MQL, the cutting area is cleaner and produces higher efficiency. The MQL technique also enables a reduction in the amount of fluid used, thereby minimizing waste and environmental impact associated with the use of conventional cutting fluids.

Vegetable-oil-based lubricants, combined with the MQL, are beneficial; however, the minimal flow rates used in MQL can limit cooling because the liquid may evaporate at elevated temperatures [27]. To address this, many studies have developed nanoparticle-based cutting fluids ("nano-cutting fluids"), since the addition of nanoparticles enhances heat-transfer performance and provides a more substantial cooling effect [28]. Extensive research has therefore focused on nanofluid-assisted machining combined with MQL spraying to improve properties, performance, and efficiency in metal cutting [29], [30]. Ongoing work continues to refine cooling strategies, particularly for heavy-duty machining. In this context, hybrid nanofluids, synthesized by dispersing at least two additives in a base cutting fluid, have gained attention because they combine complementary strengths to deliver superior overall performance. A study reported better performance across all conditions for an Al–MoS_2 hybrid than for dry cutting, base fluid, or an Al_2O_3 mono-nanofluid when turning AISI 304 [31]. Additionally, a significant improvement was observed during the turning of AISI 52100 when pure MQL, an Al_2O_3 nanofluid, and an Al–GnP hybrid were mixed [32]. Moreover, an Al–CuO hybrid outperformed dry, wet, cryogenic, pure MQL, and mono (Al_2O_3 or CuO) cooling strategies [33]. Likewise, it was found a 41.54% reduction in surface roughness compared with dry cutting and base-fluid MQL in an Al_2O_3/MoS_2 hybrid nanofluid for MQL-assisted turning of hardened AISI 420 and reported [34]. Furthermore, it was found on the tribological properties investigation of soybean oil biolubricants with the addition of Al_2O_3 and

MoS_2 additives that biolubricants with nano-hybrids can improve machining and provide better finishes [35].

However, most prior studies focusing on CuO/Graphene hybrid nanoparticles in soybean oil remain scarce, and their synergistic role in enhancing both heat transfer and tribological performance under MQL conditions has not been critically established. The combined formulation of hybrid nanoparticles, along with their application in soybean oil-based nanofluids for CNC machining under MQL conditions, has not yet been systematically investigated, which is the focus of this study. This study investigates soybean oil-based bio-lubricants enhanced with CuO, graphene, and CuO/graphene hybrid nanoparticles in 5-axis CNC milling of AISI 1045 steel. By systematically integrating CuO/graphene hybrids and correlating their thermophysical properties with machining performance, the work offers new insights into the synergistic role of hybrid nanoparticles. In contrast to previous studies that mainly examined single additives or overlooked the link between fluid properties and machining outcomes, this approach establishes a comprehensive evaluation of both aspects. The results are expected to inform the design of eco-friendly cutting fluids and support sustainable manufacturing practices.

2. Material and methods

2.1 Material

Soybean oil was used as the base oil for the preparation of cutting fluid samples. CuO and graphene nanoparticles were employed as additives, and their properties are presented in Tables 1 and 2.

Table 1. Properties of CuO

Properties	CuO
Molecular weight	Min 99%
True density	6.315 g/cm³
Insoluble substances in dilute HCl	Max 0.02%
Chloride (Cl)	Max 0.005%
Average particle size	< 55 nm

Table 2. Properties of graphene

Properties	Graphene
Type	KNG-150 Graphene Nanoplatelets
Diameter	5 µm
Thickness	<15 nm
Carbon content	>98 wt%
True density	2.25 g/cm³

Meanwhile, the material used for the experiment when applying MQL Cutting Fluid in the milling machine process is AISI 1045 steel with a workpiece size of 50 mm x 50 mm x 20 mm (L x W x H). The chemical composition and mechanical properties are shown in Tables 3 and 4. SOLID brand high-speed steel (HSS) endmill with a diameter of 8 mm and 4 flutes, the specifications of the HSS endmill used are shown in Table 5.

Table 3. Chemical composition of AISI 1045 steel

Element	C	Mn	Si	P	S	Fe
Component (%)	0.45	0.69-0.83	0.19-0.29	0.008-0.039	0.015-0.02	Balance

Table 4. Mechanical properties of AISI 1045 Steel

Mechanical Properties	AISI 1045 Steel
Ultimate Tensile Strength (MPa)	569
Yield Strength (MPa)	343
Elongation (%)	20
Modulus of Elasticity (GPa)	205
Machinability (%)	55
Shear Modulus (GPa)	80

Table 5. Specification of endmill HSS

Specification	HSS
Material	High Speed Steel
Brand	SOLID
Diameter (mm)	8
Total Length (mm)	70
Number of Cutting Edges	4 flutes

2.2 Cutting fluid sample preparation

Nano-cutting fluid tests were conducted using a two-step strategy, involving a sequence of mixing and homogenization steps [36], [37]. The sample preparation process began by mixing hybrid CuO/Graphene additive nanoparticles (0.15 wt%, comprising 0.075 wt% graphene and 0.075 wt% CuO) into soybean oil and stirring with a magnetic stirrer for 20 minutes at a rotation speed of 1250 rpm, followed by homogenization using an ultrasonic homogenizer for 30 minutes to achieve an excellent dispersion level in the cutting fluid sample. The nano-cutting fluid sample preparation and experimental design used in this study are illustrated in Figure 1 and summarized in Table 6.

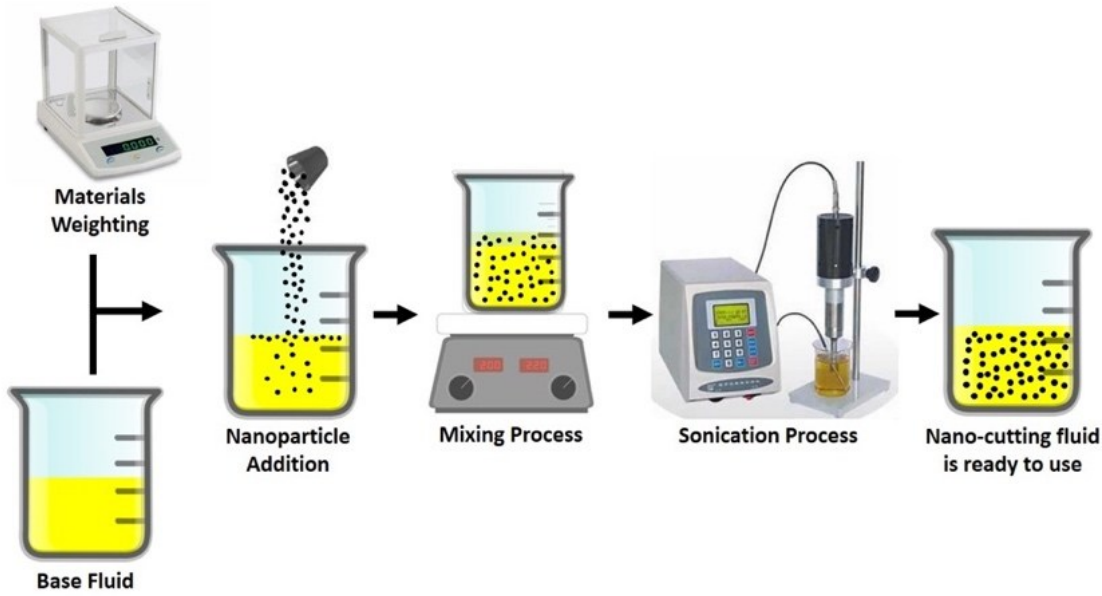

Figure 1. Cutting fluid sample preparation

Table 6. Experimental design

No.	Sample	Nanoparticles concentration (wt%)	Lubricating condition	Sample codes
1	Dry (Without cutting fluid)	-	-	Dry
2	Dromus (Commercial Cutting Fluid)	-	MQL	Dromus
3	Soybean Oil	-	MQL	Pure SO
4	Soybean Oil + CuO	0.15	MQL	SO + CuO
5	Soybean Oil + Graphene	0.15	MQL	SO + Graphene
6	Soybean Oil + Hybrid CuO/Graphene	0.15	MQL	SO + Hybrid

2.3 Experimental setup CNC milling machining

In this study, the CNC machining process was employed to identify and assess the performance of a sample of soybean oil-based cutting fluid containing CuO/Graphene hybrid additive nanoparticles. This fluid was sprayed using the MQL method. Additionally, various components of the CNC machine utilized in the experiment were also evaluated. The MQL preparation process involves a mist-shaped spraying nozzle, a compressor to apply pressure to the cutting fluid sample during machining, and a flow regulator to maintain consistent air pressure. The CNC machining scheme employing MQL is depicted in Figure 2, along with the corresponding machining parameters listed in Table 7.

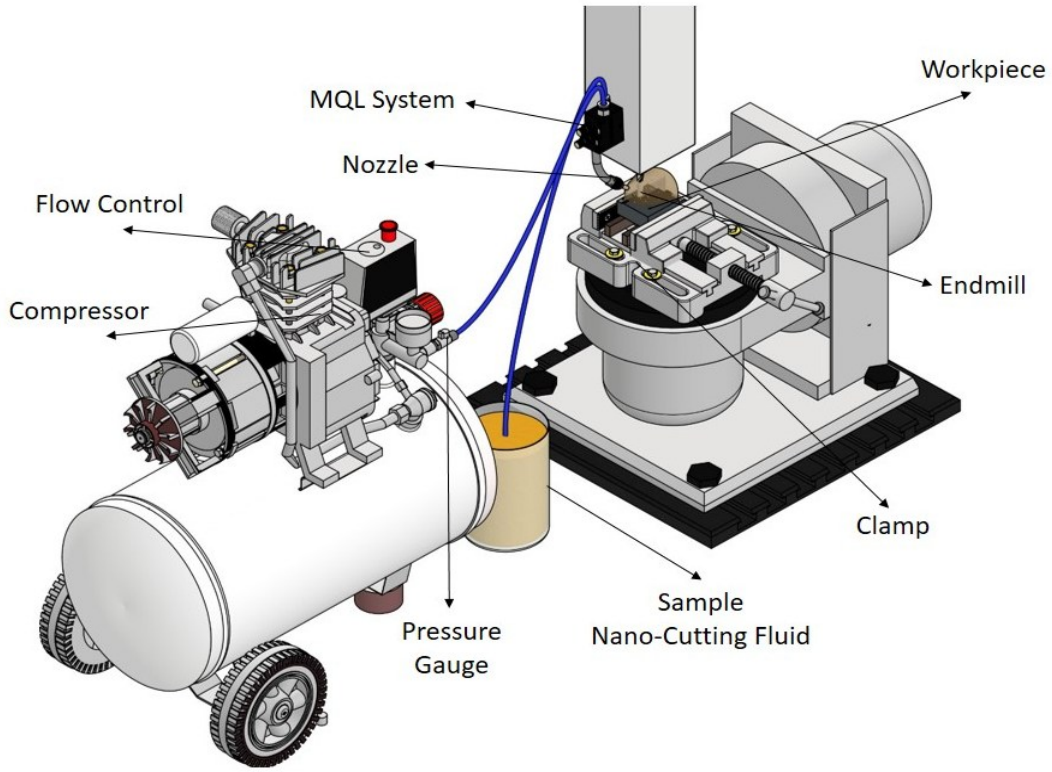

Figure 2. Schematic of milling experiment

Table 7. Milling parameter

Milling parameters	Parameter setting
Milling way	Face Milling
Tool Type	Endmill Cutter HSS Diameter 8 mm
Workpiece	AISI 1045 Steel
Spindle Speed	3000 rpm
Feed Rate	100 mm/min
Depth of Cut	1.5 mm
Cutting Speed	110 m/min
Cooling Type	MQL
MQL Nozzle Distance	20 mm
MQL Nozzle Angle	45°
MQL Pressure	4 bars

2.4 Characterization techniques

2.4.1 Characterization of additive nanoparticles

The morphology of the additive nanoparticles was examined using scanning electron microscopy (SEM) with an FEI Inspect-S50, Japan [38], [39], [40]. The phase identification and crystallite size of the additive nanoparticles were measured using X-ray diffraction (XRD) with a PANalytical Expert Pro [41], [42]. The functional groups of the additive nanoparticles was measured using a Fourier Transform Infrared (FTIR) model with an IR Prestige 21 Shimadzu [43], [44].

2.4.2 Thermophysical test of cutting fluid samples

Density of cutting fluid samples was measured using analytical digital scales at room temperature. The mass value was obtained from the weight of the sample, while the volume was measured using a pycnometer [45], [46]. Thermal conductivity testing was conducted to determine the heat transfer performance of the nano-cutting fluid sample using KD2 Pro [47]. Dynamic viscosity was measured to get the viscosity level or resistance value of the given flow to calculate the rheological value of the cutting fluid sample NDJ-8S Viscometer tool at 40°C and 100°C [48], [49]. Sedimentation testing was conducted to determine the level of separation between additive nanoparticles and soybean oil using the sedimentation method, which relies on gravity. The suspension was kept for 0, 4, 8, 12, 16, 20, 24, and 28 days. All thermophysical tests were performed three times for each formulation following standard testing and measurement procedures.

2.4.3 Rheological test of cutting fluid samples

The rheological properties of this research are used to determine the flow type of the cutting fluid, which involves studying the relationship between shear rate and shear stress. To obtain the shear rate and shear stress values, the results of the cutting fluid dynamic viscosity test are needed [50]. The following equations were applied to calculate the shear rate value (Equation 1) and the value of shear stress (Equation 2).

$$\gamma = \frac{2\omega R_c^{\,2} R_b^{\,2}}{x^2\left(R_c^{\,2} - R_b^{\,2}\right)} \tag{1}$$

Where γ is the shear rate (1/s); ω is the angular velocity (rad/s); R_c is the container radius (cm); R_b is the rotor radius (cm); and x is the radius at which the shear rate is calculated (cm).

$$\tau = \mu \times \gamma \tag{2}$$

Where τ is shear stress (Pa); μ is dynamic viscosity (mPa.s); and γ is shear rate (1/s).

2.4.4 Tribological test of cutting fluid samples

HSS endmill tool wear was examined using a Sinher Binocular optical microscope type XSZ-107 BN to determine the wear area at an interval of 4 HSS endmill flutes [51]. Then, the wear length was measured using *ImageJ* software to determine the tool wear length. This cutting tool wear was measured on the edge side based on the length of wear that occurs on that side. Surface roughness testing was conducted to assess the level of roughness on the surface of AISI 1045 workpieces resulting from the CNC milling machining process. Measurement of cutting temperature in this study was performed using a FLIR E8 Thermal Camera. Surface roughness testing was carried out on specimens machined using cutting fluid samples [52], [53]. Wear debris morphology was performed to analyze the chip characteristics of AISI 1045 machined workpieces. Wear debris morphology was performed using a scanning electron microscope FEI Inspect-S50, Japan. Chip color analysis was conducted to determine the color formed during the workpiece cutting process, as the formation of chips in the machining process can serve as an indicator to identify excessive heat in cutting and assess the performance of each cutting fluid sample. This chip color analysis was carried out using a macro camera [54].

3. Results and discussion

3.1 Additive nanoparticles characterization

3.1.1 Morphology of CuO and graphene additive nanoparticles

CuO nanoparticles were examined using scanning electron microscopy (SEM) with a magnification of 50kx, as shown in Figure 3 (a). The CuO nanoparticles exhibit a cube-like morphology, forming well-dispersed crystals that are relatively well-defined, although a high tendency for agglomeration or clumping is also observed. Particle growth due to the accumulation of a dense cube array and several significant parts of nanoparticles surrounded by smaller nanoparticles can be observed [55]. In Figure 3 (b), it is evident that graphene has a nanoplatelet structure with various morphological shapes, as indicated by the sheet accumulation pattern, which is attributed to the nanomaterial's surface energy and high surface-to-volume ratio [56]. The morphology of the characterization results is in line with the SEM test conducted by Singh et. al. [57]. Graphene nanoplatelets are typically classified as quasi-bidimensional nanostructures, similar to multi-walled carbon nanotubes. The shape of graphene nanoplatelets is not entirely flat, but instead has a crooked shape, similar to that of flower petals [58].

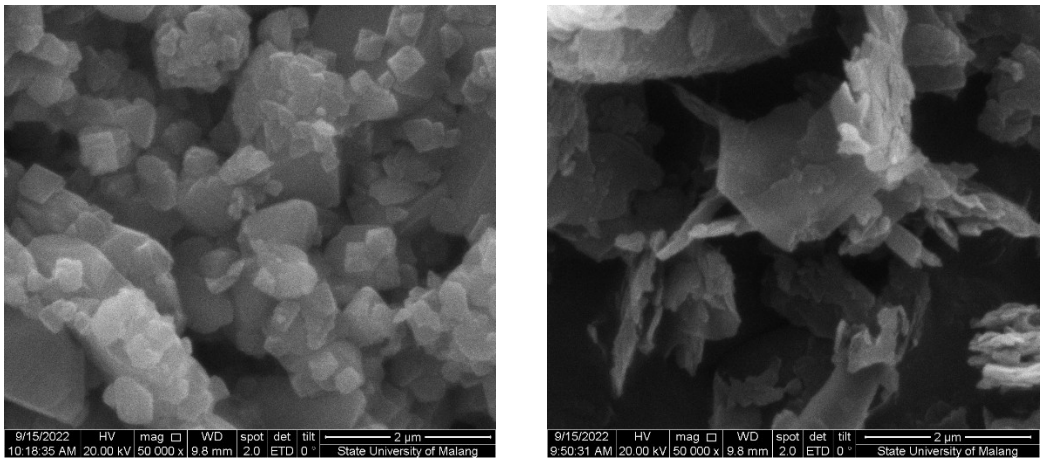

(a) (b)

Figure 3. SEM results of (a) CuO nanomaterial and (b) Graphene at 50kx magnification

3.1.2 Phase and crystallite size of CuO and graphene additive nanoparticles

Based on Figure 4 (a), the XRD result of CuO nanoparticles shows that the Copper (II) Oxide (CuO) nanomaterial has a monoclinic structure pattern with correlated peak data covering 32.5140°, 35.4513°, 38.7289°, 48.7557°, 53.4692°, 58.3112°, 61.5492°, 66.2674°. The Miller Index (hkl) at each peak is (110), (002), (111), (-202), (020), (202), (-113), (-311). The phase candidates contained in CuO nanomaterials are tenorite phases [59]. The resulting sharp diffraction peak indicates that CuO nanomaterials possess a pure monoclinic structure and exhibit high crystalline properties [60]. In addition to the peak data, an average crystallite size can be obtained from XRD testing using the Scherrer equation. For the nanomaterial CuO at position 35.4513 with a FWHM of 0.0960, the average crystallite size is 87 nm. Based on Figure 4 (b), the results of the XRD test of graphene nanomaterials show that the graphene nanomaterial has a hexagonal structure pattern with correlated peak data covering 26.4336° and 54.5347°. The Miller Index (hkl) at each peak is (002) and (004). The sharp peaks of graphene nanomaterials exhibit a large crystallite size and have a well-organized structure [61]. In addition to the peak data, an average crystal size can also be obtained from the XRD test using the Scherrer equation. At the graphene nanomaterial position of 26.4336 with a FWHM of 0.2558, the average crystal size is 31 nm.

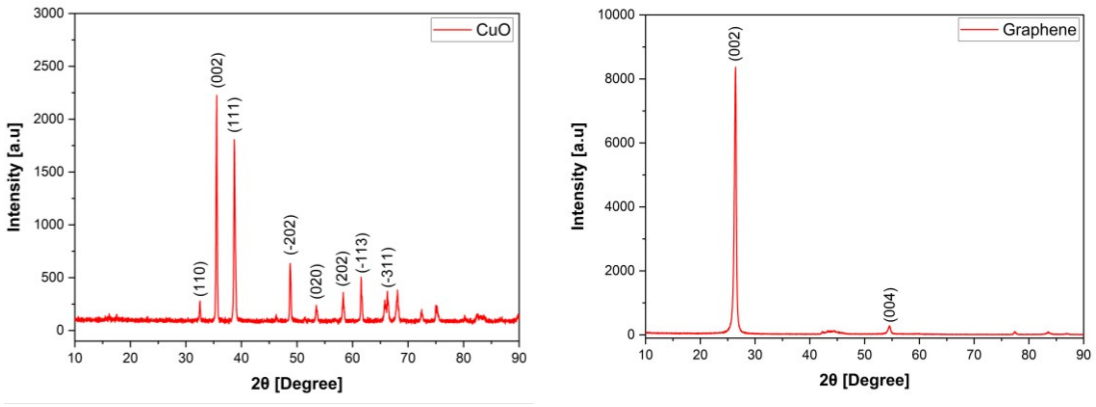

(a) (b)

Figure 4. XRD results of (a) CuO and (b) Graphene nanoparticles additives

3.1.3 Functional groups of CuO and graphene additive nanoparticles

Based on Figure 5 (a), the Fourier Transform Infrared (FTIR) graph of CuO nanomaterial shows that there are identified valleys at wavelengths of 3447 cm^{-1}, 3357 cm^{-1}, 1534 cm^{-1}, 1410 cm^{-1}, 1120 cm^{-1}, and 590 cm^{-1}. Furthermore, each valley can be analyzed, and the identified functional groups in the CuO nanomaterial are O-H, -OH, C=O, C–O, and Cu-O. Based on Figure 5 (b) of the FTIR graph of graphene nanomaterial, it is known that there are identified valleys at wavelengths of 3700 cm^{-1}, 3000 cm^{-1}, 1720 cm^{-1}, 1500 cm^{-1}, 1100 cm^{-1}, and 802 cm^{-1}. Furthermore, each valley can be analyzed, and the identified functional groups in graphene nanomaterials are O-H, C-H, C=O, C=C, C–O, and C-H, respectively (Tables 8 and 9).

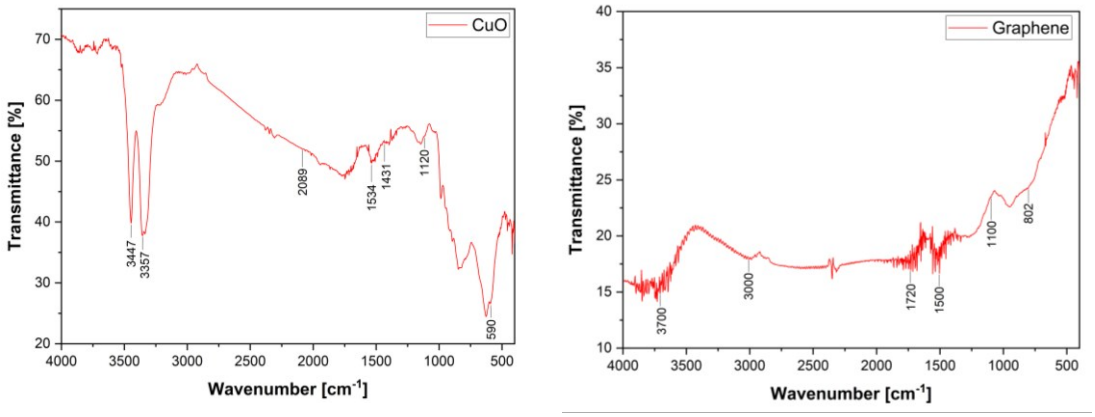

(a) (b)

Figure 5. FTIR results of (a) CuO and (b) Graphene additive nanoparticles

Table 8. Functional groups of CuO additive nanoparticles

Band	Main peak	Typical bond assignment	Reference
1	3447	O-H stretching	[62]
2	3357	O-H stretching	[63]
3	1534	-OH stretching	[64]
4	1410	C=O stretching	[65]
5	1120	C-O stretching	[63]
6	590	Cu-O stretching vibrations	[66]

Table 9. Function groups of graphene additive nanoparticles

Band	Main peak	Typical bond assignment	Reference
1	3700	O-H stretching vibrations	[67]
2	3000	C-H stretching vibrations	[68]
3	1720	C=O stretching vibrations	[69]
4	1500	C=C aromatic	[70]
5	1100	C–O stretching vibration	[68]
6	802	C-H bend vibrations	[71]

3.2 Thermophysical properties of cutting fluid samples

3.2.1 Density of cutting fluid samples

Figure 6 shows the density of the cutting fluid sample and the soybean oil sample with the addition of additive nanoparticles, which exhibits an increase in the density value. The increase in density occurs because soybean oil contains a high concentration of nanoparticles [72]. High-density values are obtained in soybean oil nanolubricants with CuO additives. The density value is influenced by several factors, including the mass, size, and properties of particles contained in a substance [73]. The results of the study conducted by Ridwan and Pamungkas [74] concluded that the density value of CuO nanoparticle is higher than that of graphene nanoparticle because the density value possessed by CuO nanoparticle is significantly higher than that of graphene nanoparticle [75].

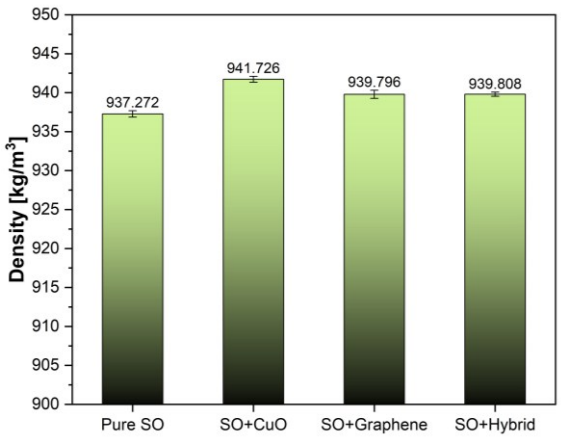

Figure 6. Density of Cutting Fluid Samples (mean ± SD, n = 3)

3.2.2 Viscosity of cutting fluid samples

Figure 7 shows the dynamic viscosity of the cutting fluid sample. The image indicates that soybean oil with additive nanoparticles has a reduced viscosity value compared to pure soybean oil. This phenomenon is caused by thixotropy, which occurs when soybean oil is subjected to loading or changes in certain conditions, such as shear stress or shear rate [76], [77]. The phenomenon of thixotropy describes the decrease in dynamic viscosity values that occurs when frictional forces or temperature changes are applied at a given time. In soybean oil, the degree of thixotropy becomes evident beyond a specific shear-rate threshold and scales mainly with additive nanoparticles concentration, though particle attributes also contribute. It supports that the viscosity value of soybean oil with graphene additive nanoparticles is higher than that of pure soybean oil [78]. The addition of CuO additives results in a lower viscosity compared to soybean oil [79].

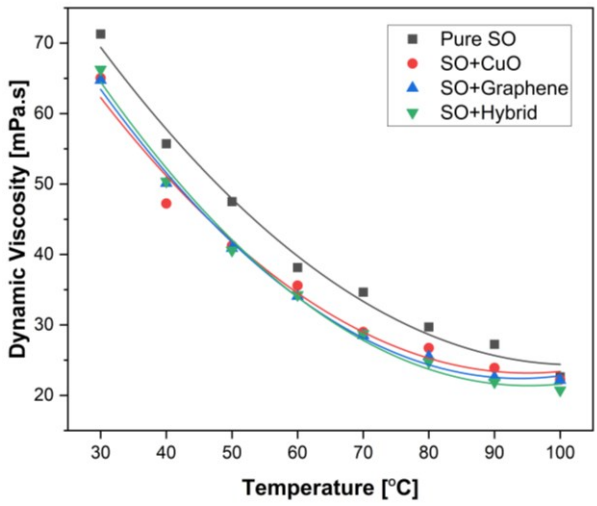

Figure 7. Dynamic viscosity of cutting fluid samples

3.2.3 Thermal conductivity of cutting fluid samples

Figure 8 has shown that the result of the thermal conductivity of the fluid that has the most outstanding value is SO+Graphene with a thermal conductivity of 0.177 W/m.K. Graphene enhances the thermal conductivity of biolubricants by acting as a high-conductivity "thermal bridge" that couples the fluid matrix and reduces interfacial (solid–liquid) thermal resistance at graphene–lubricant boundaries [80]. Its high aspect ratio and large specific surface area facilitate the formation

of continuous, phonon-mediated heat-transfer pathways, thereby improving energy transport through the suspension. The magnitude of this enhancement depends on platelet geometry, notably particle size and layer thickness, which govern pathway connectivity and coupling with the surrounding fluid [81]. In addition, Brownian motion and thermophoretic effects can further augment energy transport, complementing the 2D, high-aspect-ratio pathways established by graphene and contributing to the observed rise in effective thermal conductivity for graphene-based formulations [82]. Meanwhile, the addition of CuO additive nanoparticles to soybean oil can only slightly increase the thermal conductivity value in line with research conducted by Rajaganapathy et. al. [83]. In the case of SO+Hybrid, the thermal conductivity did not surpass that of SO+Graphene, suggesting that the anticipated synergistic enhancement was not realized. This limitation is likely due to particle–particle interactions, where CuO agglomeration disrupts the uniform dispersion of graphene, thereby reducing interfacial contact and effective phonon transport. Consequently, instead of complementing each other, the two nanoparticles compete within the fluid matrix, resulting in diminished thermal transport efficiency. Additional nanoparticles produce Brownian motion, which is the random motion of particles suspended in a fluid (liquid or gas) caused by collisions with atoms or molecules of the fluid. This movement increases the transfer of energy more efficiently across the fluid, thereby enhancing heat transfer within the fluid. The addition of nanoparticles with the right concentration will increase the thermal conductivity value of the base fluid [84]. However, if the concentration of nanoparticles is too high, it will limit the Brownian motion of nanoparticles in the base fluid, causing agglomeration and reducing thermal conductivity [85].

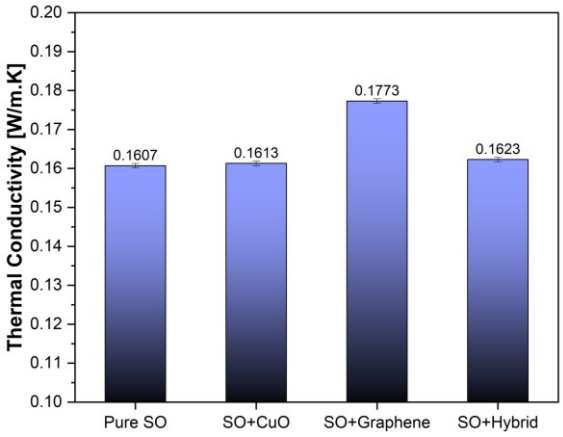

Figure 8. Thermal Conductivity of Cutting Fluid Samples (mean ± SD, n = 3)

3.2.4 Sedimentation

The 28-day sedimentation test (Figure 9) shows that SO+CuO exhibits visibly greater sedimentation than cutting fluids without CuO. Among all formulations, SO+CuO has the most considerable sediment fraction. CuO nanoparticles (99% purity) have a density of 6.4 g/cm^3 [86], whereas graphene nanoparticles (99.5% carbon) have a density of 2.0 g/cm^3 [76]. Higher particle density increases the gravitational settling rate, thereby reducing the dispersion stability of nanolubricants [74]. In parallel, Brownian motion, while beneficial to thermal transport, can modify interparticle dynamics. Coupled with gravity and density mismatch, these factors promote settling for heavy oxides, such as CuO [82]. In addition, metal-oxide particles such as CuO are generally hydrophilic and disperse poorly in low-polarity oils unless surface-functionalized (e.g., oleic-acid capping) to provide steric stabilization; otherwise, van der Waals attraction promotes agglomeration and subsequent sedimentation [87], [88]. By contrast, graphene's high-aspect-ratio, two-dimensional platelets experience greater hydrodynamic drag than near-spherical oxides of

comparable volume, which reduces the settling velocity; this shape-dependent drag effect is well documented [89].

(a) (b)

Figure 9. (a) 0-Day Sedimentation Results and (b) 28-Day Sedimentation Results

3.3 Rheology of cutting fluid samples

The results of the calculation of shear rate and shear stress values to determine the rheological properties of cutting fluid samples at temperatures of 40°C and 100°C in this study are shown in Figure 10. Based on the comparison between the shear rate and shear stress values in soybean oil and cutting fluid samples with different additive nanoparticles, at temperatures of 40°C and 100°C, as shown, they exhibit Newtonian flow behavior. Newtonian fluids exhibit consistent performance in lubrication, particularly in cutting fluid applications where loads and speeds fluctuate. This consistency can maintain surface separation, helping to prevent excessive friction and wear during the machining process [90].

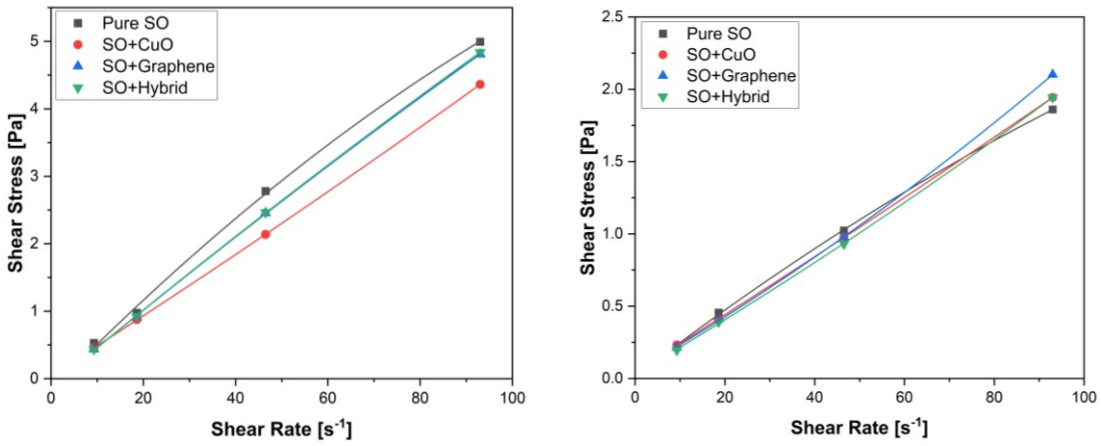

(a) (b)

Figure 10. Rheological properties of cutting fluids at temperatures (a) 40°C and (b) 100°C

3.4 Cutting fluid performance on CNC milling machining

3.4.1 Surface roughness

Figure 11 shows that the highest surface roughness value was obtained in dry conditions with a surface roughness value of 2.18 µm. Lower surface roughness was achieved by SO+Graphene using the MQL method compared to the dry condition method in the machining process application [91]. Graphene has a layered structure that provides a weak van der Waals force, thus creating a low shear field. The high specific surface area of graphene enables it to quickly penetrate the surface between the workpiece and the cutting tool [92]. Additionally, graphene exhibits excellent thermal conductivity and lubrication properties. This can be attributed to the fact that graphene additives

enhance the lubrication and cooling performance of tribofilms formed in the cutting zone, thereby reducing the friction coefficient and influencing the surface roughness value [93]. The SO+Hybrid samples exhibit a higher surface roughness compared to graphene nanoparticles. This occurs because CuO nanoparticles have a high tendency to agglomerate. Agglomeration can prevent free motion and easily push it out of the friction surface, thus preventing nanoparticles from penetrating the friction surface. This shows that nanoparticles with flat sheets have better tribological performance compared to crystal-shaped nanoparticles [74].

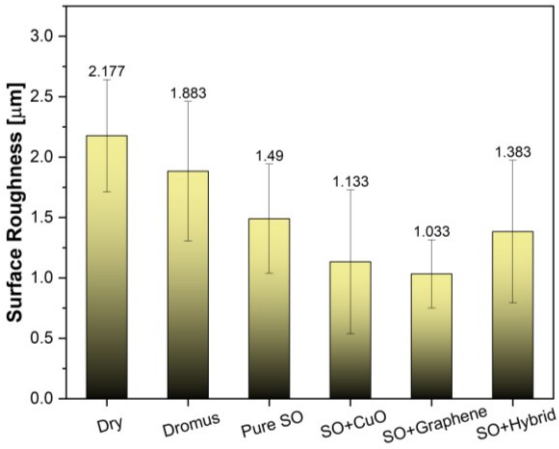

Figure 11. Surface roughness of AISI 1045 Steel after machining (mean ± SD, n = 3)

3.4.2 Tool wear

Figures 12 and 13 show the wear of the endmill and flute endmill after the machining process. Based on the figure, the highest tool wear value is obtained in dry conditions, with a tool wear of 0.300 mm. The lowest tool wear value was obtained with SO+Graphene, with a tool wear value of 0.05 mm. The application of the MQL method in machining applications can reduce the mass of tool wear compared to using the dry condition method [94], [95]. The vegetable oil-based MQL method has a lower friction force, resulting in a lower tool wear value compared to the dry condition method, due to the fatty acids that enhance lubrication properties [72]. The SO+Graphene sample shows excellent anti-friction and stable performance, as graphene nanoparticles have a hexagonal molecular structure, which shows that graphene-based cutting fluid has the best lubrication stability and abrasive resistance [96], [97]. Graphene nanoparticles play a role in reducing friction. The thickness of graphene nanoparticles can form a tribofilm that acts as a protective layer, preventing direct contact with friction surfaces (as illustrated in Figure 14). In addition, the two-dimensional sheet shape of graphene nanoparticles creates a low shear field, as well as improved thermal conductivity, which leads to enhanced surface quality, reduced wear, and better heat dissipation performance [98]. Vegetable oils can form a lubricating layer on the contact surface between the workpiece and the cutting tool, providing a smooth surface for the cutting process. Graphene nanomaterials can improve lubrication further. The air pressure exerted can transport the nanolubricant towards the workpiece. When the cutting tool comes into contact, it can effectively weaken the affinity between the workpiece material and the tool surface, thus further inhibiting the adhesion of the chip and reducing abrasive adhesion [99]. Figure 12 shows a graph indicating that the SO+hybrid has higher tool wear compared to graphene and CuO additives. This occurs because CuO nanomaterials are unevenly distributed on the surface and can clump. This is due to agglomeration caused by low dispersibility, resulting in lower wear protection [100].

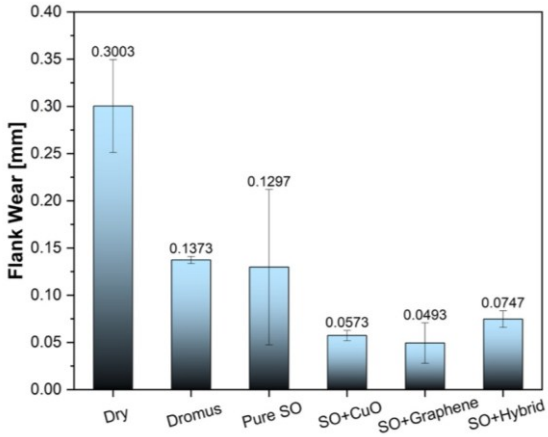

Figure 12. Tool wear of endmill after machining (mean ± SD, n = 3)

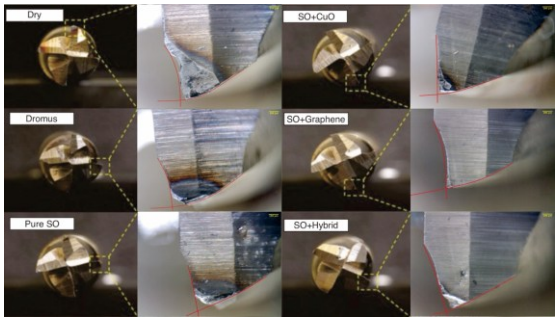

Figure 13. Endmill flute wear macro photo

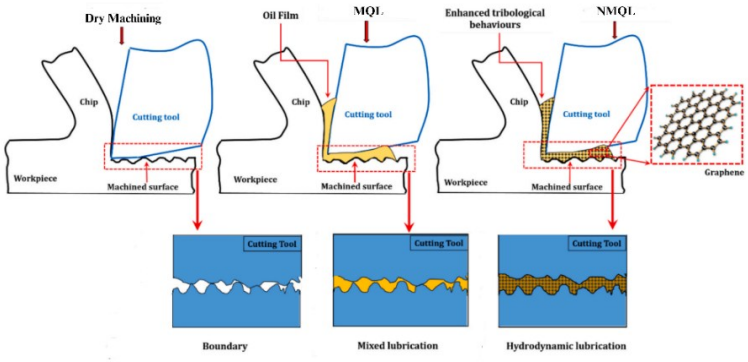

Figure 14. Tribofilm illustration in the machining process. Reproduce from [92]

3.4.3 Cutting temperature

Based on Figures 15 and 16, it is shown that the addition of nanoparticles can lower the machining temperature. For instance, the cutting temperature decreased from 139.7 °C under dry conditions to 85.4 °C with Dromus, 77.8 °C with pure SO, 53.4 °C with SO+CuO, and reached the lowest value of 46.1 °C with SO+Graphene, before slightly increasing to 68.3 °C with SO+Hybrid. This indicates that nanoparticles play a significant role in improving the thermal management of the cutting zone. The most abundant work of nanoparticles in oil, apart from increasing the thermal conductivity value in the base fluid, also serves as a protective medium on the surface of the object, counteracting the frictional force produced and generating energy to offset the frictional force [101]. The reduction in cutting temperature achieved by using nano-cutting fluids based on vegetable oils and a mixture of additive nanoparticles is attributed to the combination of good thermal conductivity and oil properties in the center of the machine handle, particularly at the

contact surfaces of the cutting device, chips, and workpiece [102]. These trends are consistent with the tool wear and surface roughness data presented in Figures 11 and 12, where the lowest flank wear of 0.049 mm and surface roughness of 1.033 µm were achieved with SO+Graphene, coinciding with the lowest recorded cutting temperature. High viscosity also promotes a more uniform distribution of the cutting fluid under MQL conditions, contributing to the formation of an effective thermal protective layer. However, this effect must be complemented by a sufficiently high thermal conductivity to enhance heat dissipation [103]. Furthermore, the dispersed nanoparticles form a thin film at the cutting interface, acting as rolling elements that reduce friction and contribute to smoother machining [104].

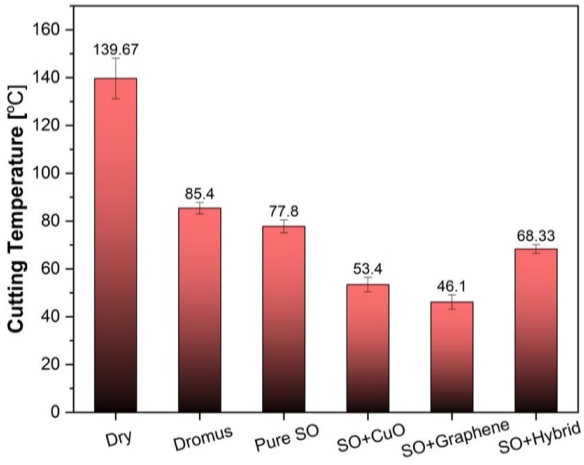

Figure 15. Cutting temperature test results (mean ± SD, n = 3)

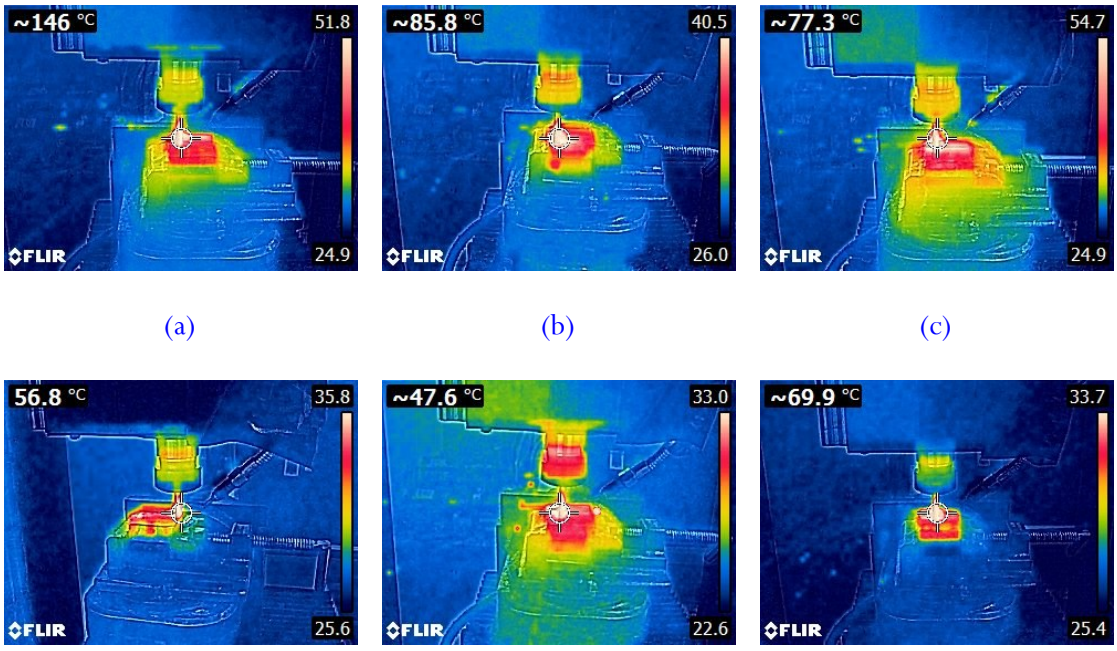

(a) (b) (c)

(d) (e) (f)

Figure 16. Temperature measurement during the machining process under the following conditions: (a) dry, (b) dromus, (c) pure SO, (d) SO+CuO, (e) SO+Graphene, and (f) SO+Hybrid

3.4.4 Chip morphology analysis

Figure 17 shows the SEM results of the wear debris morphology, presented in various views (normal, general, and magnified). Tests conducted using dry media or under dry conditions showed a rough chip surface shape and small, irregular serrations, whereas those using dromus media showed a rough chip surface shape and irregular serrations. Tests conducted using MQL media, such as pure SO and SO+Graphene, showed a smooth surface shape of the chip with irregular, small serrations. In contrast, when using SO+CuO and SO+Hybrid, the surface indicated slightly rough chips with irregular fine serrations. Differences in the morphological shape of wear debris, such as shape and serrations, can reflect the quality of machining [105]. Specifically, dry machining exhibited C-type chips with coarse serrations, correlating with the highest surface roughness of 2.177 µm and tool wear of 0.300 mm. In contrast, SO+Graphene produced smoother chips with minimal serrations, consistent with its lowest flank wear of 0.049 mm and roughness of 1.033 µm. The intermediate behavior observed in SO+Hybrid demonstrates that although hybrid nanoparticles improve tribological behavior, their synergistic effect does not surpass the single graphene addition. Dry conditions have the most jagged and irregular chip shape due to high friction, causing the temperature in the cutting zone to increase significantly [92]. In contrast, chips with a small serration rate are caused by slight friction, which increases the heat transfer process in the cutting zone. The use of MQL and nano-MQL methods proves good cooling [106]. Soybean oil, when used with the MQL method, can reduce plastic deformation and exhibit even feeding marks. The CuO has a ball bearing capability that can fill gaps to minimize interaction and the ability to carry a considerable load. Additionally, CuO exhibits minimal shear resistance, which reduces friction at surface contact [107]. The wear debris formed by the addition of CuO nanomaterials in soybean oil exhibits tiny serrations and a slightly smooth surface. Graphene has a layered structure, high thermal conductivity, high mechanical strength, and easy sliding ability, which enables it to function as a lubricant and reduce wear in various tribology applications [108].

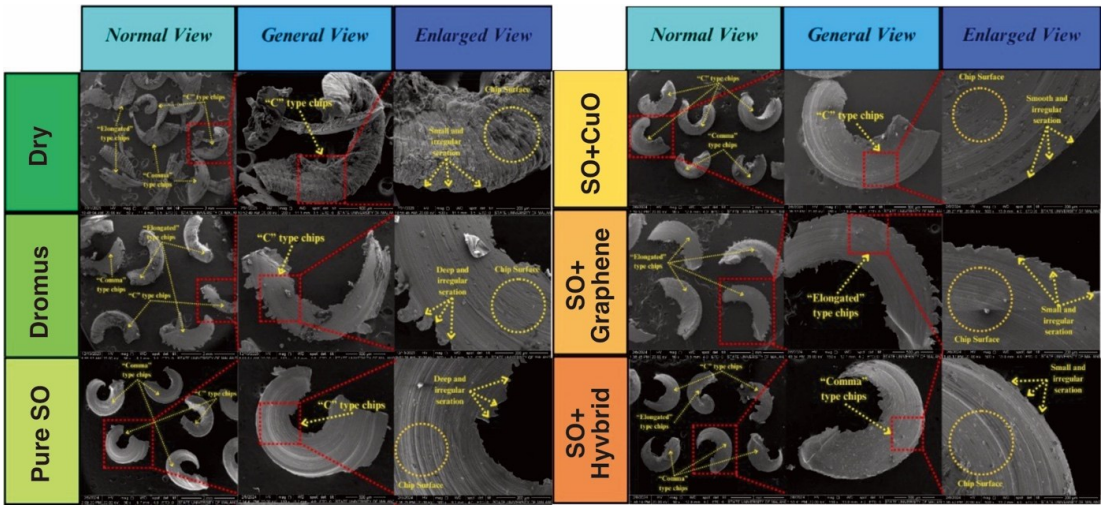

Figure 17. Morphological results of wear debris

3.4.5 Chip color analysis

Figure 18 shows the result of chip color evolution under different lubrication conditions, which reflects the thermal state of the cutting zone. In dry machining, the chips exhibited a dark brown color, indicating severe oxidation and high cutting temperature (139.7 °C). Similarly, Dromus also produced brown chips, consistent with limited cooling capacity. Pure SO resulted in black wear debris, suggesting partial carbonization due to insufficient heat removal [109]. In contrast, the addition of CuO nanoparticles yielded golden-colored chips, attributed to its moderate thermal

conductivity and partial load-carrying "ball-bearing" effect. The best performance was observed with SO+Graphene, where chips retained a bright silver color, indicating effective heat dissipation (46.1 °C) and minimal oxidation [110]. Finally, the SO+Hybrid condition produced brownish chips, indicating less effective cooling compared to SO+Graphene. Overall, the silver chip color obtained with graphene nanolubricants correlates with the lowest measured tool wear (0.049 mm) and surface roughness (1.033 µm), confirming its superior tribological and thermal performance [111]. The excellent thermal conductivity of graphene surpasses that of most carbon-based materials, enabling better heat dissipation and lower frictional forces [112].

Figure 18. Chip color after application of cutting fluid samples in CNC milling

3.4.6 Benchmarking of soybean oil-based nano-cutting fluid under MQL: Cross-study comparison

Table 10 situates our milling with MQL results within representative literature. Within our dataset, SO+Graphene consistently delivers lower roughness, wear, and cutting temperature than SO+CuO and the CuO/graphene hybrid (≈22-25% lower Ra, ≈14-34% lower VB, and ≈14-33% lower T). Compared with other vegetable-oil systems, graphene shows competitive wear resistance with moderate Ra; additives such as $CaCO_3$ or hBN can achieve very low Ra in some studies, mostly at the cost of higher wear, however. It indicates a roughness-wear trade-off. Turning entries frequently report lower Ra due to different kinematics and parameter windows, so they are not directly comparable to milling. Graphene likely forms a low-shear, heat-spreading tribolayer, whereas CuO's aggregation and particle–particle interactions in the hybrid can disrupt tribolayer continuity, limiting synergy. Practical takeaway: for milling-MQL, where thermal control and tool life dominate, SO+Graphene is a strong candidate; for finishing that prioritizes ultra-smooth surfaces, $CaCO_3$/hBN systems may be considered with attention to wear.

Table 10. Cross-study comparison of machining performance metrics: surface roughness, flank wear, and cutting temperature for nano-lubricants under minimum quantity lubrication (MQL)

Sample	Machining and Lubrication Condition	Surface Roughness (µm)	Tool Wear (mm)	Cutting temperature (°C)	Ref.
Soybean Oil + 0.15wt% CuO	Milling-MQL	1.33	0.0573	53.4	
Soybean Oil + 0.15wt% Graphene	Milling-MQL	1.033	0.0493	46.1	
Soybean Oil + 0.15wt% Hybrid CuO/Graphene	Milling-MQL	1.383	0.0747	68.33	
Mineral Oil/Water + 1.2wt% Al-GNP (85:15)	Turning-MQL	0.65	-	-	[32]
Comercial Cutting Fluid + 0.6wt% Al-CuO	Turning-MQL	~0.7	-	~35	[33]
Synthetic Oil + 0.4vol% Al_2O_3 + 0.2vol% MoS_2	Turning-MQL	~0.38	~0.05	~240	[34]
Synthetic Oil + 0.2vol% MWCNT + 0.4vol% Al_2O_3	Turning-MQL	~0.48	~0.16	~285	[34]
Palm Oil + 0.15wt% MWCNT	Milling-MQL	1.27	0.059	-	[113]
Palm Oil + 0.15wt% MWCNT/CuO	Milling-MQL	1.4	0.107	-	[113]
Canola Oil + 0.15wt% CaCO3	Milling-MQL	0.83	0.073	35.77	[72]
Soybean Oil + 0.15wt% CaCO3	Milling-MQL	0.93	0.064	34.27	[72]
Canola Oil + 0.15 wt% hBN	Milling-MQL	0.86	0.120	35.43	[72]
Corn Oil + 0.15wt% MWCNT	Milling-MQL	-	0.044	-	[114]

4. Conclusion

This work systematically evaluated soybean oil (SO) nanolubricants containing CuO, graphene, and CuO/graphene hybrids for MQL-assisted CNC milling of AISI 1045, linking thermophysical and rheological properties to machining responses (surface roughness, flank wear, and cutting temperature). Based on the experimental findings, the conclusions are as follows:

a. The graphene formulation consistently performed best, achieving the lowest roughness (Ra = 1.033 µm), wear (VB = 0.049 mm), and temperature (T = 46.1 °C). The CuO/graphene hybrid improved performance versus base fluids but did not surpass graphene, indicating limited synergy under the present SO–MQL conditions. Thermophysically, graphene enhanced effective thermal conductivity and supported heat evacuation, while CuO increased density and exhibited lower dispersion stability over 28 days. Rheology at 40 °C and 100 °C was Newtonian across all formulations, ensuring predictable lubrication behavior at the applied shear rates.

b. The application of soybean oil-based nanolubricants offers a clear, environmentally friendly alternative to conventional cutting fluids. Compared to Dry and Dromus conditions, the nanoparticle-reinforced oils provided stable lubrication, reduced thermal loading, and minimized tool/workpiece damage, supporting both machining efficiency and ecological responsibility. SO+Graphene exhibited the strongest balance of performance and sustainability, while SO+CuO and SO+Hybrid also delivered tangible improvements over Pure SO, reinforcing their practicality as green lubricants.

c. These results carry significant implications for advancing sustainable manufacturing. The consistent superiority of SO+Graphene, together with the synergistic potential of SO+Hybrid, highlights the importance of nanoparticle selection and formulation strategy. Future studies should address long-term dispersion stability, scalability in industrial CNC applications, and optimization of hybrid nanoparticle ratios to fully harness thermal–tribological synergies.

d. Limitations include possible agglomeration/sedimentation over time, a restricted process window (single setup/ratio), and the absence of confirmatory surface imaging. Practically, scale-up and cost (dispersion energy, surfactant, and inline filtration to prevent nozzle clogging) warrant attention. Future work will optimize surfactant and CuO: graphene ratios, conduct closed-loop long-term stability tests with simple monitoring, and perform a lean techno-economic assessment to support industrial adoption.

Author's declaration

Author contribution

Agus Setiawan: Funding acquisition, Investigation, Validation, Writing - Original Draft. **Poppy Puspitasari**: Conceptualization, Formal analysis, Resources, Visualization, Writing - Original Draft. **Mohammad Tauviqirrahman**: Formal analysis, Investigation, Validation, Writing - Review & Editing. **Diki Dwi Pramono**: Methodology, Data Curation, Formal analysis, Visualization, Writing - Original Draft. **Haipan Salam**: Investigation, Validation, Writing - Review & Editing.

Funding statement

This work was supported by Universitas Pendidikan Indonesia through the Riset Kolaborasi Indonesia (RKI) funding scheme (Reference No. 726/UN40/PT.01.01/2025).

Data Availability

All data supporting the findings of this study are available from the authors upon reasonable request. The data include both original datasets generated during the research.

Acknowledgements

The authors would like to express their sincere gratitude to technicians at Mechanical and Industrial Engineering of Universitas Negeri Malang for their support in preparing samples and their characterization. The authors would also like to thank Professor Andoko of Universitas Negeri Malang for his valuable discussion, which has improved this paper.

Competing interest

There are no conflicts of interest in this research.

Ethical clearance

This research does not involve humans as subjects; thus, approval from the ethics committee was not required.

AI statement

The article is the author's original work. The authors have thoroughly reviewed the accuracy and relevance of the statements in relation to the study's topic and data, and no AI-generated content has been included in the manuscript.

Publisher's and Journal's note

Universitas Negeri Padang as the publisher, and Editor of Teknomekanik state that there is no conflict of interest towards this article publication.

References

[1] Z. Duan *et al.*, "Milling Force Model for Aviation Aluminum Alloy: Academic Insight and Perspective Analysis," *Chinese Journal of Mechanical Engineering*, vol. 34, no. 1, p. 18, Dec. 2021, https://doi.org/10.1186/s10033-021-00536-9

[2] V. Baldin *et al.*, "Dry and MQL Milling of AISI 1045 Steel with Vegetable and Mineral-Based Fluids," *Lubricants*, vol. 11, no. 4, p. 175, Apr. 2023, https://doi.org/10.3390/lubricants11040175

[3] J. M., P. K. M., and A. R., "Effect of LN2 and CO2 coolants in milling of 55NiCrMoV7 steel," *J Manuf Process*, vol. 53, pp. 318–327, May 2020, https://doi.org/10.1016/j.jmapro.2020.02.040

[4] Margono, Muhammad Kozin, D. Setiadhi, Hassan Khamis Hassan, and Rajeshkumar Lakshminarasimhan, "Development of Titanium Nitride-Based Coatings for Wear Resistant Materials: A Review," *Mechanics Exploration and Material Innovation*, vol. 1, no. 3, pp. 102–119, Aug. 2024, https://doi.org/10.21776/ub.memi.2024.001.03.5

[5] L. Tang *et al.*, "Biological Stability of Water-Based Cutting Fluids: Progress and Application," *Chinese Journal of Mechanical Engineering*, vol. 35, no. 1, p. 3, Dec. 2022, https://doi.org/10.1186/s10033-021-00667-z

[6] P. Shah, N. Khanna, and Chetan, "Comprehensive machining analysis to establish cryogenic LN2 and LCO2 as sustainable cooling and lubrication techniques," *Tribol Int*, vol. 148, p. 106314, Aug. 2020, https://doi.org/10.1016/j.triboint.2020.106314

[7] M. Sarikaya *et al.*, "Cooling techniques to improve the machinability and sustainability of light-weight alloys: A state-of-the-art review," *J Manuf Process*, vol. 62, pp. 179–201, Feb. 2021, https://doi.org/10.1016/j.jmapro.2020.12.013

[8] N. Khanna *et al.*, "Review on design and development of cryogenic machining setups for heat resistant alloys and composites," *J Manuf Process*, vol. 68, pp. 398–422, Aug. 2021, https://doi.org/10.1016/j.jmapro.2021.05.053

[9] L. R. Silva, E. C. S. Corrêa, J. R. Brandão, and R. F. de Ávila, "Environmentally friendly manufacturing: Behavior analysis of minimum quantity of lubricant - MQL in grinding process," *J Clean Prod*, vol. 256, p. 103287, May 2020, https://doi.org/10.1016/j.jclepro.2013.01.033

[10] G. W. A. Kui, S. Islam, M. M. Reddy, N. Khandoker, and V. L. C. Chen, *Recent progress and evolution of coolant usages in conventional machining methods: a comprehensive review*, vol. 119, no. 1–2. Springer London, 2022. https://doi.org/10.1007/s00170-021-08182-0

[11] B. Sen, M. Mia, G. M. Krolczyk, U. K. Mandal, and S. P. Mondal, *Eco-Friendly Cutting Fluids in Minimum Quantity Lubrication Assisted Machining: A Review on the Perception of Sustainable*

Manufacturing, vol. 8, no. 1. Korean Society for Precision Engineering, 2021. https://doi.org/10.1007/s40684-019-00158-6

[12] X. Wang *et al.*, "Vegetable oil-based nanofluid minimum quantity lubrication turning: Academic review and perspectives," *J Manuf Process*, vol. 59, no. March, pp. 76–97, 2020, https://doi.org/10.1016/j.jmapro.2020.09.044

[13] R. Teti, D. M. D'Addona, and T. Segreto, "Microbial-based cutting fluids as bio-integration manufacturing solution for green and sustainable machining," *CIRP J Manuf Sci Technol*, vol. 32, pp. 16–25, 2021, https://doi.org/10.1016/j.cirpj.2020.09.016

[14] J. Zhang *et al.*, "Convective Heat Transfer Coefficient Model Under Nanofluid Minimum Quantity Lubrication Coupled with Cryogenic Air Grinding Ti–6Al–4V," *International Journal of Precision Engineering and Manufacturing-Green Technology*, vol. 8, no. 4, pp. 1113–1135, Jul. 2021, https://doi.org/10.1007/s40684-020-00268-6

[15] X. Luo, S. Wu, D. Wang, Y. Yun, Q. An, and C. Li, "Sustainable development of cutting fluids: The comprehensive review of vegetable oil," *J Clean Prod*, vol. 473, p. 143544, Oct. 2024, https://doi.org/10.1016/j.jclepro.2024.143544

[16] A. H. Elsheikh, M. A. Elaziz, S. R. Das, T. Muthuramalingam, and S. Lu, "A new optimized predictive model based on political optimizer for eco-friendly MQL-turning of AISI 4340 alloy with nano-lubricants," *J Manuf Process*, vol. 67, no. April, pp. 562–578, 2021, https://doi.org/10.1016/j.jmapro.2021.05.014

[17] M. Jamil *et al.*, "Sustainable milling of Ti–6Al–4V: A trade-off between energy efficiency, carbon emissions and machining characteristics under MQL and cryogenic environment," *J Clean Prod*, vol. 281, p. 125374, Jan. 2021, https://doi.org/10.1016/j.jclepro.2020.125374

[18] H. Hegab, U. Umer, M. Soliman, and H. A. Kishawy, "Effects of nano-cutting fluids on tool performance and chip morphology during machining Inconel 718," *International Journal of Advanced Manufacturing Technology*, vol. 96, no. 9–12, pp. 3449–3458, 2018, https://doi.org/10.1007/s00170-018-1825-0

[19] A. S. Araújo Junior, W. F. Sales, R. B. da Silva, E. S. Costa, and Á. Rocha Machado, "Lubri-cooling and tribological behavior of vegetable oils during milling of AISI 1045 steel focusing on sustainable manufacturing," *J Clean Prod*, vol. 156, pp. 635–647, Jul. 2017, https://doi.org/10.1016/j.jclepro.2017.04.061

[20] R. Roy and S. Prasad, "Comparative study of mineral and soya bean oil at faulty temperature for transformer application," *IOP Conf Ser Mater Sci Eng*, vol. 1120, no. 1, p. 012028, Mar. 2021, https://doi.org/10.1088/1757-899X/1120/1/012028

[21] I. Stanciu, "Rheological Behavior of Biodegradable Lubricants," *Oriental Journal of Chemistry*, vol. 35, no. 2, pp. 684–688, Apr. 2019, https://doi.org/10.13005/ojc/350224

[22] D. Yu. Pimenov *et al.*, "Improvement of machinability of Ti and its alloys using cooling-lubrication techniques: a review and future prospect," *Journal of Materials Research and Technology*, vol. 11, pp. 719–753, Mar. 2021, https://doi.org/10.1016/j.jmrt.2021.01.031

[23] V. S. Sharma, M. Dogra, and N. M. Suri, "Cooling techniques for improved productivity in turning," *Int J Mach Tools Manuf*, vol. 49, no. 6, pp. 435–453, May 2009, https://doi.org/10.1016/j.ijmachtools.2008.12.010

[24] M. K. Gupta *et al.*, "Experimental characterisation of the performance of hybrid cryo-lubrication assisted turning of Ti–6Al–4V alloy," *Tribol Int*, vol. 153, p. 106582, Jan. 2021, https://doi.org/10.1016/j.triboint.2020.106582

[25] A. Eltaggaz, Z. Said, and I. Deiab, "An integrated numerical study for using minimum quantity lubrication (MQL) when machining austempered ductile iron (ADI)," *International Journal on Interactive Design and Manufacturing*, vol. 14, no. 3, pp. 747–758, 2020, https://doi.org/10.1007/s12008-020-00662-z

[26] B. L. Tai, D. A. Stephenson, R. J. Furness, and A. J. Shih, "Minimum quantity lubrication (MQL) in automotive powertrain machining," *Procedia CIRP*, vol. 14, pp. 523–528, 2014, https://doi.org/10.1016/j.procir.2014.03.044

[27] M. Sarıkaya and A. Güllü, "Multi-response optimization of minimum quantity lubrication parameters using Taguchi-based grey relational analysis in turning of difficult-to-cut alloy Haynes 25," *J Clean Prod*, vol. 91, pp. 347–357, Mar. 2015, https://doi.org/10.1016/j.jclepro.2014.12.020

[28] K. K. Asogwa, F. Mebarek-Oudina, and I. L. Animasaun, "Comparative Investigation of Water-Based Al2O3 Nanoparticles Through Water-Based CuO Nanoparticles Over an Exponentially Accelerated Radiative Riga Plate Surface via Heat Transport," *Arab J Sci Eng*, vol. 47, no. 7, pp. 8721–8738, Jul. 2022, https://doi.org/10.1007/s13369-021-06355-3

[29] X. Bai, C. Li, L. Dong, and Q. Yin, "Experimental evaluation of the lubrication performances of different nanofluids for minimum quantity lubrication (MQL) in milling Ti-6Al-4V," *International Journal of Advanced Manufacturing Technology*, vol. 101, no. 9–12, pp. 2621–2632, 2019, https://doi.org/10.1007/s00170-018-3100-9

[30] L. Ben Said, L. Kolsi, K. Ghachem, M. Almeshaal, and C. Maatki, *Application of nanofluids as cutting fluids in machining operations: a brief review*, vol. 13, no. 6. Springer International Publishing, 2022. https://doi.org/10.1007/s13204-021-02140-8

[31] A. K. Sharma, R. K. Singh, A. R. Dixit, and A. K. Tiwari, "Novel uses of alumina-MoS2 hybrid nanoparticle enriched cutting fluid in hard turning of AISI 304 steel," *J Manuf Process*, vol. 30, pp. 467–482, Dec. 2017, https://doi.org/10.1016/j.jmapro.2017.10.016

[32] A. M. Khan *et al.*, "Energy-based cost integrated modelling and sustainability assessment of Al-GnP hybrid nanofluid assisted turning of AISI52100 steel," *J Clean Prod*, vol. 257, p. 120502, Jun. 2020, https://doi.org/10.1016/j.jclepro.2020.120502

[33] A. Thakur, A. Manna, and S. Samir, "Performance Evaluation of Different Environmental Conditions on Output Characteristics During Turning of EN-24 Steel," *International Journal of Precision Engineering and Manufacturing*, vol. 20, no. 10, pp. 1839–1849, Oct. 2019, https://doi.org/10.1007/s12541-019-00179-w

[34] Ç. V. Yıldırım, Ş. Şirin, T. Kıvak, and M. Sarıkaya, "A comparative study on the tribological behavior of mono&proportional hybrid nanofluids for sustainable turning of AISI 420 hardened steel with cermet tools," *J Manuf Process*, vol. 73, pp. 695–714, Jan. 2022, https://doi.org/10.1016/j.jmapro.2021.11.044

[35] R. Kumar and R. K. Gautam, "Tribological investigation of sunflower and soybean oil with metal oxide nanoadditives," *Biomass Convers Biorefin*, vol. 14, no. 2, pp. 2389–2401, Jan. 2024, https://doi.org/10.1007/s13399-022-02411-6

[36] A. Nugroho *et al.*, "A Comprehensive Investigation of Low Proportion TiO2-POE Nanolubricant Stability for Residential Air Conditioning System Application," 2023, pp. 147–163. https://doi.org/10.1007/978-981-19-4425-3_15

[37] A. S. Al-Janabi, M. Hussin, M. Z. Abdullah, and M. A. Ismail, "Effect of CTAB surfactant on the stability and thermal conductivity of mono and hybrid systems of graphene and FMWCNT nanolubricant," *Colloids Surf A Physicochem Eng Asp*, vol. 648, no. April, p. 129275, 2022, https://doi.org/10.1016/j.colsurfa.2022.129275

[38] X. Bai, J. Jiang, C. Li, L. Dong, H. M. Ali, and S. Sharma, "Tribological Performance of Different Concentrations of Al2O3 Nanofluids on Minimum Quantity Lubrication Milling," *Chinese Journal of Mechanical Engineering (English Edition)*, vol. 36, no. 1, 2023, https://doi.org/10.1186/s10033-022-00830-0

[39] R. N. Elshaer and K. M. Ibrahim, "Effect of cold deformation and heat treatment on microstructure and mechanical properties of TC21 Ti alloy," *Transactions of Nonferrous Metals Society of China (English Edition)*, vol. 30, no. 5, pp. 1290–1299, 2020, https://doi.org/10.1016/S1003-6326(20)65296-7

[40] P. Puspitasari, A. Ayu Permanasari, M. Ilman Hakimi Chua Abdullah, D. Dwi Pramono, and O. Jaya Silaban, "Tribology Characteristic of Ball Bearing SKF RB-12.7/G20W using

SAE 5W-30 Lubricant with Carbon-Based Nanomaterial Addition," *Tribology in Industry*, vol. 45, no. 4, pp. 664–675, Dec. 2023, https://doi.org/10.24874/ti.1538.09.23.11

[41] D. D. Pramono and P. Puspitasari, "Comparison of physicochemical properties of hydroxyapatite from scallop shell synthesized by wet chemical method with and without sonication process," in *Proceedings of the International Conference on Green Engineering & Technology 2022 (IConGETech 2022)*, Arau: AIP Conference Proceedings, Nov. 2024, p. 040034. https://doi.org/10.1063/5.0199107

[42] P. Trihutomo, P. Puspitasari, M. B. Radja, and M. R. Busono, "Synthesis and Characterization of Nitrogen-Doped Activated Carbon for Lithium Battery Anode Applications," *Journal of Mechanical Engineering Science and Technology (JMEST)*, vol. 7, no. 1, p. 20, 2023, https://doi.org/10.17977/um016v7i12023p020

[43] D. D. Pramono, P. Puspitasari, A. A. Permanasari, S. Sukarni, and A. Wahyudiono, "Effect of Sintering Time on Porosity and Compressibility of Calcium Carbonate from Amusium Pleuronectes (Scallop Shell)," in *AIP Conference Proceedings*, American Institute of Physics Inc., May 2023. https://doi.org/10.1063/5.0120990

[44] D. D. Pramono, P. Puspitasari, H. Suryanto, Y. Zakaria, and M. J. Ghazali, "Synergistic effects of sonication duration and calcination temperature on the structural, physicochemical and bioactivity of biogenic nano-hydroxyapatite from scallop shells for bone repair applications," *Mater Chem Phys*, vol. 348, p. 131571, Jan. 2026, https://doi.org/10.1016/j.matchemphys.2025.131571

[45] M. Gupta, V. Singh, R. Kumar, and Z. Said, "A review on thermophysical properties of nanofluids and heat transfer applications," *Renewable and Sustainable Energy Reviews*, vol. 74, no. February, pp. 638–670, 2017, https://doi.org/10.1016/j.rser.2017.02.073

[46] P. Puspitasari, D. D. Pramono, D. N. Fiansyah, A. A. Permanasari, N. Mufti, and J. A. Razak, "Biodiesel production from waste cooking oil using calcium oxide derived from scallop shell waste," *Clean Energy*, vol. 8, no. 2, pp. 113–126, Apr. 2024, https://doi.org/10.1093/ce/zkae005

[47] M. U. Sajid and H. M. Ali, "Thermal conductivity of hybrid nanofluids: A critical review," *Int J Heat Mass Transf*, vol. 126, pp. 211–234, Nov. 2018, https://doi.org/10.1016/j.ijheatmasstransfer.2018.05.021

[48] A. Bhattad, "Review on viscosity measurement: devices, methods and models," *J Therm Anal Calorim*, vol. 148, no. 14, pp. 6527–6543, Jul. 2023, https://doi.org/10.1007/s10973-023-12214-0

[49] C. Pownraj and A. Valan Arasu, "Effect of dispersing single and hybrid nanoparticles on tribological, thermo-physical, and stability characteristics of lubricants: a review," *J Therm Anal Calorim*, vol. 143, no. 2, pp. 1773–1809, Jan. 2021, https://doi.org/10.1007/s10973-020-09837-y

[50] S. V. Sujith, A. K. Solanki, and R. S. Mulik, "Experimental evaluation on rheological behavior of Al2O3-pure coconut oil nanofluids," *J Mol Liq*, vol. 286, p. 110905, Jul. 2019, https://doi.org/10.1016/j.molliq.2019.110905

[51] A. Eltaggaz, S. Ali, K. Badwal, and I. Deiab, "Influence of nanoparticle concentration in nanofluid MQL on cutting forces, tool wear, chip morphology when milling of Inconel 718," *The International Journal of Advanced Manufacturing Technology*, vol. 129, no. 3–4, pp. 1787–1800, Nov. 2023, https://doi.org/10.1007/s00170-023-12393-y

[52] M. A. Makhesana, K. M. Patel, and P. J. Bagga, "Evaluation of Surface Roughness, Tool Wear and Chip Morphology during Machining of Nickel-Based Alloy under Sustainable Hybrid Nanofluid-MQL Strategy," *Lubricants*, vol. 10, no. 11, p. 315, Nov. 2022, https://doi.org/10.3390/lubricants10110315

[53] M. D. Riyanto, A. Andoko, and H. Suryanto, "Effect of Current and Pulse-on Time on Material Removal Rate and Surface Roughness of Tungsten Carbide in Electric Discharge Machine Die-sinking," *Journal of Mechanical Engineering Science and Technology (JMEST)*, vol. 7, no. 1, p. 39, Jun. 2023, https://doi.org/10.17977/um016v7i12023p039

[54] G. Sharma *et al.*, "Advanced Materials Research Chair , Department of Chemistry , College of Science , School of Electrical and Computer Science Engineering , Shoolini University , Solan School of Chemistry & Physics , University of KwaZulu-Natal , Pietermaritzburg," *J King Saud Univ Sci*, 2017, https://doi.org/10.1016/j.jksus.2017.06.012

[55] I. Z. Luna, L. N. Hilary, A. M. S. Chowdhury, M. A. Gafur, N. Khan, and R. A. Khan, "Preparation and Characterization of Copper Oxide Nanoparticles Synthesized via Chemical Precipitation Method," *OAlib*, vol. 02, no. 03, pp. 1–8, 2015, https://doi.org/10.4236/oalib.1101409

[56] S. A. Ebrahim, E. Pradeep, S. Mukherjee, and N. Ali, "Rheological behavior of dilute graphene-water nanofluids using various surfactants: An experimental evaluation," *J Mol Liq*, vol. 370, p. 120987, 2023, https://doi.org/10.1016/j.molliq.2022.120987

[57] S. Singh, V. K. Srivastava, and R. Prakash, "Influences of carbon nanofillers on mechanical performance of epoxy resin polymer," *Appl Nanosci*, vol. 5, no. 3, pp. 305–313, Mar. 2015, https://doi.org/10.1007/s13204-014-0319-0

[58] G. Carotenuto *et al.*, "Mechanical properties of low-density polyethylene filled by graphite nanoplatelets," *Nanotechnology*, vol. 23, no. 48, p. 485705, Dec. 2012, https://doi.org/10.1088/0957-4484/23/48/485705

[59] A. F. Zedan, A. T. Mohamed, M. S. El-Shall, S. Y. AlQaradawi, and A. S. AlJaber, "Tailoring the reducibility and catalytic activity of CuO nanoparticles for low temperature CO oxidation," *RSC Adv*, vol. 8, no. 35, pp. 19499–19511, 2018, https://doi.org/10.1039/C8RA03623C

[60] A. A. Abdel-Rehim, S. Akl, and S. Elsoudy, "Investigation of the Tribological Behavior of Mineral Lubricant Using Copper Oxide Nano Additives," *Lubricants*, vol. 9, no. 2, p. 16, Feb. 2021, https://doi.org/10.3390/lubricants9020016

[61] I.-M. Low, H. M. Albetran, and M. Degiorgio, "Structural Characterization of Commercial Graphite and Graphene Materials," *Journal of Nanotechnology and Nanomaterials*, no. 1, Jun. 2020, https://doi.org/10.33696/Nanotechnol.1.005

[62] S. Suresh, S. Karthikeyan, and K. Jayamoorthy, "FTIR and multivariate analysis to study the effect of bulk and nano copper oxide on peanut plant leaves," *Journal of Science: Advanced Materials and Devices*, vol. 1, no. 3, pp. 343–350, 2016, https://doi.org/10.1016/j.jsamd.2016.08.004

[63] Y. K. Phang *et al.*, "Green synthesis and characterization of CuO nanoparticles derived from papaya peel extract for the photocatalytic degradation of palm oil mill effluent (POME)," *Sustainability (Switzerland)*, vol. 13, no. 2, pp. 1–15, 2021, https://doi.org/10.3390/su13020796

[64] E. Badetti *et al.*, "Interaction between copper oxide nanoparticles and amino acids: Influence on the antibacterial activity," *Nanomaterials*, vol. 9, no. 5, 2019, https://doi.org/10.3390/nano9050792

[65] A. El-Trass, H. Elshamy, I. El-Mehasseb, and M. El-Kemary, "CuO nanoparticles: Synthesis, characterization, optical properties and interaction with amino acids," *Appl Surf Sci*, vol. 258, no. 7, pp. 2997–3001, 2012, https://doi.org/10.1016/j.apsusc.2011.11.025

[66] A. Rahman, A. Ismail, D. Jumbianti, S. Magdalena, and H. Sudrajat, "Synthesis Of Copper Oxide Nano Particles By Using Phormidium cyanobacterium," *Indonesian Journal of Chemistry*, vol. 9, no. 3, pp. 355–360, 2010, https://doi.org/10.22146/ijc.21498

[67] A. Paydayesh, F. Pashaei Soorbaghi, A. Aref Azar, and A. Jalali-Arani, "Electrical conductivity of graphene filled PLA/PMMA blends: Experimental investigation and modeling," *Polym Compos*, vol. 40, no. 2, pp. 704–715, 2019, https://doi.org/10.1002/pc.24722

[68] K. H. Solangi *et al.*, "Experimental investigation of heat transfer performance and frictional loss of functionalized GNP-based water coolant in a closed conduit flow," *RSC Adv*, vol. 6, no. 6, pp. 4552–4563, 2016, https://doi.org/10.1039/c5ra23998b

[69] Y. Song *et al.*, "Enhancing the thermal, electrical, and mechanical properties of silicone rubber by addition of graphene nanoplatelets," *Mater Des*, vol. 88, pp. 950–957, 2015, https://doi.org/10.1016/j.matdes.2015.09.064

[70] D. Ratih, R. Siburian, and Andriayani, "The performance of graphite/n-graphene and graphene/n-graphene as electrode in primary cell batteries," *Rasayan Journal of Chemistry*, vol. 11, no. 4, pp. 1649–1656, 2018, https://doi.org/10.31788/RJC.2018.1145007

[71] P. Lamichhane *et al.*, "Thermal stability and optoelectronic behavior of polyaniline/GNP (graphene nanoplatelets) nanocomposites," 2022.

[72] P. Puspitasari *et al.*, "Experimental Evaluation of Biolubricant with Additive Nanoparticle Calcium Carbonate (CaCO3) from Scallop Shell Waste as Cutting Fluids using Minimum Quantity Lubrication (MQL) in CNC Milling Process," *FME Transactions*, vol. 52, no. 2, pp. 319–334, 2024, https://doi.org/10.5937/fme2402319P

[73] R. M. Ridwan and G. P. Pamungkas, "Prototipe Densitometer Berdasarkan Perbedaan Gaya Buoyancy Berbasis Sensor Piezoresistif dan Sensor Infra-Red Thermometer," *Jurnal Otomasi Kontrol dan Instrumentasi*, vol. 9, no. 1, p. 21, May 2018, https://doi.org/10.5614/joki.2017.9.1.3

[74] N. F. Azman, S. Samion, M. A. A. Moen, M. K. Abdul Hamid, and M. N. Musa, "The anti-wear and extreme pressure performance of CuO and graphite nanoparticles as an additive in palm oil," *International Journal of Structural Integrity*, vol. 10, no. 5, pp. 714–725, Oct. 2019, https://doi.org/10.1108/IJSI-03-2019-0026

[75] A. Belli, A. Mobili, T. Bellezze, F. Tittarelli, and P. Cachim, "Evaluating the Self-Sensing Ability of Cement Mortars Manufactured with Graphene Nanoplatelets, Virgin or Recycled Carbon Fibers through Piezoresistivity Tests," *Sustainability*, vol. 10, no. 11, p. 4013, Nov. 2018, https://doi.org/10.3390/su10114013

[76] R. G. Larson and Y. Wei, "A review of thixotropy and its rheological modeling," *J Rheol (N Y N Y)*, vol. 63, no. 3, pp. 477–501, May 2019, https://doi.org/10.1122/1.5055031

[77] S. S. Sanukrishna, S. Vishnu, and M. Jose Prakash, "Experimental investigation on thermal and rheological behaviour of PAG lubricant modified with SiO 2 nanoparticles," *J Mol Liq*, vol. 261, pp. 411–422, Jul. 2018, https://doi.org/10.1016/j.molliq.2018.04.066

[78] C. George Catalin, R. Alexandru, G. Constantin, R. Irina, and D. Lorena, "Influence of Additive concentration in Soybean Oil on Rheological and tribological Behavior," *INCAS BULLETIN*, vol. 10, no. 4, pp. 35–43, Dec. 2018, https://doi.org/10.13111/2066-8201.2018.10.4.4

[79] Y. G. Bi and H. C. He, "Preparation of Biodiesel from Soybean Oil by Ultrasound-Assisted Transesterification," *Adv Mat Res*, vol. 773, pp. 188–192, Sep. 2013, https://doi.org/10.4028/www.scientific.net/AMR.773.188

[80] B. Wang *et al.*, "Thermal conductivity and mechanical properties enhancement of <scp>CF</scp> / <scp>PPBESK</scp> thermoplastic composites by introducing graphene," *Polym Compos*, vol. 43, no. 5, pp. 2736–2745, May 2022, https://doi.org/10.1002/pc.26570

[81] W. H. Danial and Z. Abdul Majid, "Recent advances on the enhanced thermal conductivity of graphene nanoplatelets composites: a short review," *Carbon Letters*, vol. 32, no. 6, pp. 1411–1424, Oct. 2022, https://doi.org/10.1007/s42823-022-00371-5

[82] K. Ramesh, F. Mebarek-Oudina, and B. Souayeh, *Mathematical Modelling of Fluid Dynamics and Nanofluids*. Boca Raton: CRC Press, 2023. https://doi.org/10.1201/9781003299608

[83] C. Rajaganapathy, D. Vasudevan, and S. Murugapoopathi, "Tribological and rheological properties of palm and brassica oil with inclusion of CuO and TiO2 additives," *Mater Today Proc*, vol. 37, no. Part 2, pp. 207–213, 2020, https://doi.org/10.1016/j.matpr.2020.05.032

[84] D. Rahmadiawan, N. Aslfattahi, N. Nasruddin, R. Saidur, A. Arifutzzaman, and H. A. Mohammed, "MXene Based Palm Oil Methyl Ester as an Effective Heat Transfer Fluid,"

Journal of Nano Research, vol. 68, pp. 17–34, Jun. 2021, https://doi.org/10.4028/www.scientific.net/JNanoR.68.17

[85] M. Seyhan, C. L. Altan, B. Gurten, and S. Bucak, "The effect of functionalized silver nanoparticles over the thermal conductivity of base fluids," *AIP Adv*, vol. 7, no. 4, Apr. 2017, https://doi.org/10.1063/1.4979554

[86] F. Hekmatipour, M. A. Akhavan-Behabadi, B. Sajadi, and M. Fakoor-Pakdaman, "Mixed convection heat transfer and pressure drop characteristics of the copper oxide-heat transfer oil (CuO-HTO) nanofluid in vertical tube," *Case Studies in Thermal Engineering*, vol. 10, pp. 532–540, Sep. 2017, https://doi.org/10.1016/j.csite.2017.09.009

[87] Y. Chen, P. Renner, and H. Liang, "Dispersion of Nanoparticles in Lubricating Oil: A Critical Review," *Lubricants*, vol. 7, no. 1, p. 7, Jan. 2019, https://doi.org/10.3390/lubricants7010007

[88] V. S. Mello, E. A. Faria, S. M. Alves, and C. Scandian, "Enhancing Cuo nanolubricant performance using dispersing agents," *Tribol Int*, vol. 150, p. 106338, Oct. 2020, https://doi.org/10.1016/j.triboint.2020.106338

[89] E. E. Michaelides and Z. Feng, "Review—Drag Coefficients of Non-Spherical and Irregularly Shaped Particles," *J Fluids Eng*, vol. 145, no. 6, Jun. 2023, https://doi.org/10.1115/1.4057019

[90] H. F. George and F. Qureshi, "Newton's Law of Viscosity, Newtonian and Non-Newtonian Fluids," in *Encyclopedia of Tribology*, Boston, MA: Springer US, 2013, pp. 2416–2420. https://doi.org/10.1007/978-0-387-92897-5_143

[91] A. Pal, S. S. Chatha, and H. S. Sidhu, "Assessing the lubrication performance of various vegetable oil-based nano-cutting fluids via eco-friendly MQL technique in drilling of AISI 321 stainless steel," *Journal of the Brazilian Society of Mechanical Sciences and Engineering*, vol. 44, no. 4, pp. 1–26, 2022, https://doi.org/10.1007/s40430-022-03442-w

[92] M. N. Babu, V. Anandan, Ç. V. Yıldırım, M. D. Babu, and M. Sarıkaya, "Investigation of the characteristic properties of graphene-based nanofluid and its effect on the turning performance of Hastelloy C276 alloy," *Wear*, vol. 510–511, no. April, 2022, https://doi.org/10.1016/j.wear.2022.204495

[93] M. Li, T. Yu, R. Zhang, L. Yang, H. Li, and W. Wang, "MQL milling of TC4 alloy by dispersing graphene into vegetable oil-based cutting fluid," *International Journal of Advanced Manufacturing Technology*, vol. 99, no. 5–8, pp. 1735–1753, 2018, https://doi.org/10.1007/s00170-018-2576-7

[94] S. Khatai, R. Kumar, A. Kumar Sahoo, and A. Panda, "Investigation on tool wear and chip morphology in hard turning of EN 31 steel using AlTiN-PVD coated carbide cutting tool," *Mater Today Proc*, vol. 59, pp. 1810–1816, 2022, https://doi.org/10.1016/j.matpr.2022.04.387

[95] D. Gasni, D. Rahmadiawan, R. Irwansyah, and A. E. Khalid, "Composite of Carboxymethyl Cellulose/MXene and Span 60 as Additives to Enhance Tribological Properties of Bio-Lubricants," *Lubricants*, vol. 12, no. 3, p. 78, Mar. 2024, https://doi.org/10.3390/lubricants12030078

[96] X. Cui *et al.*, "Tribological properties under the grinding wheel and workpiece interface by using graphene nanofluid lubricant," *The International Journal of Advanced Manufacturing Technology*, vol. 104, no. 9–12, pp. 3943–3958, Oct. 2019, https://doi.org/10.1007/s00170-019-04129-8

[97] D. Rahmadiawan *et al.*, "Exploring the tribological properties and wear morphology of high-temperature MXene/CMC nanofluid as a high-performance and environmentally lubricant," 2025, p. 040002. https://doi.org/10.1063/5.0243045

[98] J. Huang, J. Tan, H. Fang, F. Gong, and J. Wang, "Tribological and wear performances of graphene-oil nanofluid under industrial high-speed rotation," *Tribol Int*, vol. 135, no. March, pp. 112–120, 2019, https://doi.org/10.1016/j.triboint.2019.02.041

[99] B. Wang, Q. Yang, J. Deng, N. Hou, X. Wang, and M. Wang, "Effect of graphene nanoparticles and sulfurized additives to MQL for the machining of Ti-6Al-4 V," *The International Journal of Advanced Manufacturing Technology*, vol. 119, no. 5–6, pp. 2911–2921, Mar. 2022, https://doi.org/10.1007/s00170-021-08348-w

[100] M. Gulzar *et al.*, "Improving the AW/EP ability of chemically modified palm oil by adding CuO and MoS2 nanoparticles," *Tribol Int*, vol. 88, pp. 271–279, Aug. 2015, https://doi.org/10.1016/j.triboint.2015.03.035

[101] L. Peña-Parás, D. Maldonado-Cortés, M. Rodríguez-Villalobos, A. G. Romero-Cantú, and O. E. Montemayor, "Enhancing tool life, and reducing power consumption and surface roughness in milling processes by nanolubricants and laser surface texturing," *J Clean Prod*, vol. 253, 2020, https://doi.org/10.1016/j.jclepro.2019.119836

[102] S. Hu *et al.*, "Nanoparticle-enhanced coolants in machining: mechanism, application, and prospects," *Frontiers of Mechanical Engineering*, vol. 18, no. 4, p. 53, Dec. 2023, https://doi.org/10.1007/s11465-023-0769-8

[103] M. Çelik, A. Çakır Şencan, Ş. Şirin, B. Erdoğan, and C. Şencan, "Effect of hBN and SDS added vegetable based cutting fluid application on the performance of turning Ti6Al4V alloys: A Comparative analysis with Taguchi and ANN approaches," *Mater Chem Phys*, vol. 322, p. 129552, Aug. 2024, https://doi.org/10.1016/j.matchemphys.2024.129552

[104] W. Safiei, M. M. Rahman, A. R. Yusoff, M. N. Arifin, and W. Tasnim, "Effects of SiO2-Al2O3-ZrO2 Tri-hybrid Nanofluids on Surface Roughness and Cutting Temperature in End Milling Process of Aluminum Alloy 6061-T6 Using Uncoated and Coated Cutting Inserts with Minimal Quantity Lubricant Method," *Arab J Sci Eng*, vol. 46, no. 8, pp. 7699–7718, 2021, https://doi.org/10.1007/s13369-021-05533-7

[105] J. Kouam, V. Songmene, M. Balazinski, and P. Hendrick, "Effects of minimum quantity lubricating (MQL) conditions on machining of 7075-T6 aluminum alloy," *The International Journal of Advanced Manufacturing Technology*, vol. 79, no. 5–8, pp. 1325–1334, Jul. 2015, https://doi.org/10.1007/s00170-015-6940-6

[106] M. Günay and M. E. Korkmaz, "Understanding the Relationship between Surface Quality and Chip Morphology under Sustainable Cutting Environments," *Materials*, vol. 17, no. 8, p. 1826, Apr. 2024, https://doi.org/10.3390/ma17081826

[107] A. Roushan, U. S. Rao, P. Sahoo, K. Patra, and S. S. Rawat, "Wear behavior of AlTiN coated WC tools in micromilling of Ti6Al4V alloy using vegetable oil-based nanofluids," *Tribol Int*, vol. 188, p. 108825, Oct. 2023, https://doi.org/10.1016/j.triboint.2023.108825

[108] R. Singh, J. S. Dureja, M. Dogra, M. K. Gupta, and M. Mia, "Influence of graphene-enriched nanofluids and textured tool on machining behavior of Ti-6Al-4V alloy," *The International Journal of Advanced Manufacturing Technology*, vol. 105, no. 1–4, pp. 1685–1697, Nov. 2019, https://doi.org/10.1007/s00170-019-04377-8

[109] Y. Abidi, "Relationship between surface roughness and chip morphology when turning hardened steel," *Production Engineering Archives*, vol. 26, no. 3, pp. 92–98, Sep. 2020, https://doi.org/10.30657/pea.2020.26.19

[110] R. Vishal, K. Nimel Sworna Ross, G. Manimaran, and B. K. Gnanavel, "Impact on Machining of AISI H13 Steel Using Coated Carbide Tool under Vegetable Oil Minimum Quantity Lubrication," *Mater Perform Charact*, vol. 8, no. 1, pp. 527–537, Jan. 2019, https://doi.org/10.1520/MPC20190154

[111] S.-H. Chen and M.-S. Gao, "The study of chip characteristics and tool wear in milling of SKD61 mold steel," *Journal of Mechanical Science and Technology*, vol. 36, no. 6, pp. 2817–2824, Jun. 2022, https://doi.org/10.1007/s12206-022-0514-y

[112] A. M. M. Ibrahim, W. Li, H. Xiao, Z. Zeng, Y. Ren, and M. S. Alsoufi, "Energy conservation and environmental sustainability during grinding operation of Ti–6Al–4V alloys via eco-friendly oil/graphene nano additive and Minimum quantity lubrication," *Tribol Int*, vol. 150, p. 106387, Oct. 2020, https://doi.org/10.1016/j.triboint.2020.106387

[113] P. Puspitasari, A. A. Permanasari, A. M. H S Lubis, M. Z. Ardiansyah, D. D. Pramono, and M. Ilman Hakimi Chua Abdullah, "Thermophysical, rheological and tribological properties of palm oil with hybrid CuO/MWCNT additive nanoparticles as cutting fluid on CNC machining," *Jurnal Tribologi*, vol. 9, No. 2, pp. 268–293, 2025. https://doi.org/10.17977/um016v9i22025p317

[114] M. A. Abdiyar *et al.*, "Enhanced Tribological Performance of Canola Oil-Based Nano-Cutting Fluids with Hexagonal Boron Nitride (h-BN) Nanoparticle Additives under the Minimum Quantity Lubrication (MQL) Method," *Malaysian Journal on Composites Science and Manufacturing*, vol. 17, no. 1, pp. 1–20, Jul. 2025. https://doi.org/10.37934/mjcsm.17.1.120

Nomenclature

Symbol	Descriptions	
L	Length	[mm]
W	Width	[mm]
H	Height	[mm]
γ	Shear rate	[1/s]
ω	Angular velocity	[rad/s]
R_c	Container radius	[cm]
R_b	Rotor radius	[cm]
x	Radius at which the shear rate is calculated	[cm]
τ	Shear stress	[Pa]
μ	Dynamic viscosity	[mPa.s]
FWHM	Full width at half maximum	